



## C-MEMS for the Manufacture of 3D Microbatteries

Chunlei Wang,<sup>a,z</sup> Lili Taherabadi,<sup>a</sup> Guangyao Jia,<sup>a</sup> Marc Madou,<sup>a</sup> Yuting Yeh,<sup>b</sup>  
and Bruce Dunn<sup>b</sup>

<sup>a</sup>Department of Mechanical and Aerospace Engineering University of California, Irvine,  
Irvine, California 92697-3975, USA

<sup>b</sup>Department of Materials Science and Engineering, University of California, Los Angeles, Los Angeles,  
California 90095-1595, USA

We have demonstrated that carbon-microelectromechanical systems (C-MEMS), in which patterned photoresist is pyrolyzed in inert environment at high temperature, constitutes a powerful approach to building 3D carbon microelectrode arrays for 3D microbattery applications. High aspect ratio carbon posts (>10:1) are achieved by pyrolyzing SU-8 negative photoresist in a simple one step process. Lithium can be reversibly charged and discharged into these C-MEMS electrodes. Because of the additional volume of the posts, higher capacities are achieved with the 3D array electrodes as compared to unpatterned carbon films with the same projected electrode area. These novel electrode arrays represent one of the critical components for 3D batteries, which may be interconnected with C-MEMS leads to enable smart power management schemes.  
© 2004 The Electrochemical Society. [DOI: 10.1149/1.1798151] All rights reserved.

Manuscript submitted January 16, 2004; revised manuscript received April 27, 2004. Available electronically October 19, 2004.

Highly ordered graphite, as well as hard and soft carbons, are used extensively as the negative electrodes of commercial Li-ion batteries.<sup>1,2</sup> The high energy density values reported for these Li batteries are generally based on the performance of larger cells with capacities of up to several ampere-hours. For small microbatteries, with applications in miniature portable electronic devices, such as cardiac pacemakers, hearing aids, smart cards, and remote sensors, the achievable power and energy densities do not scale favorably because packaging and internal battery hardware determine the overall size and mass of the completed battery to a large extent. Therefore, further improvements in advanced microbatteries are intimately linked to the availability of new materials and the development of novel battery designs. One approach to overcome the size and energy density deficiencies of 2D microbatteries is to develop 3D battery architectures based on specially designed arrays composed of high aspect ratio 3D electrode elements.<sup>3,4</sup> White and colleagues have calculated that for a 3D microbattery which has electrode arrays with a 50:1 aspect ratio (height/width), the expected capacity may be 3.5 times higher than that of a conventional 2D battery design with the same areal footprint.<sup>3</sup> The key challenge in fabricating 3D microbatteries based on carbon negative electrodes is in achieving high aspect ratio (>10:1) electrodes so that the areal footprint of a 3D battery can be less than 1 cm<sup>2</sup> without compromising capacity.<sup>4</sup> This paper provides the first report of the fabrication and lithium intercalation properties of high aspect ratio 3D carbon electrode arrays.

### Carbon-Microelectromechanical Systems

Our work in carbon-microelectromechanical systems (C-MEMS) suggests that C-MEMS might provide an interesting material and microfabrication solution to the battery miniaturization problem. In C-MEMS, photoresist is patterned by photolithography and subsequently pyrolyzed at high temperatures in an oxygen-free environment. By changing the lithography conditions, soft and hard baking time and temperature, and pyrolysis time, temperature, and environment, C-MEMS permit a wide variety of interesting new MEMS applications that employ structures having a wide variety of shapes, resistivity and mechanical properties. In the current case we used this technique to yield high aspect ratio carbon electrodes for microbatteries. The advantages of using photoresists as the starting material for carbon electrodes include the fact that photoresists can be patterned by photolithography techniques resulting in much finer features than possible with the more traditional silkscreening of carbon inks and, because photoresists are very controlled and reproducible materials, more reproducible carbon electrode behavior can be

expected (benefiting electrochemical performance of sensors, batteries, etc). Hence, complex-shaped, very fine, accurate and reproducible carbon electrodes can be manufactured. In our earlier work we demonstrated that the photoresist derived carbon electrodes show excellent electrochemical kinetics comparable to that of glassy carbon for selected electrochemical reactions in aqueous and nonaqueous electrolytes.<sup>5-7</sup> C-MEMS can be used for both the current collector and the electrodes, as illustrated in Fig. 1a, and thus provide the basis for fabricating 3D battery architectures. Until recently, the C-MEMS features we were able to fabricate were low aspect ratio structures with thicknesses less than 10 μm. As an example, in Fig. 1b we show a low aspect ratio C-MEMS battery structure, in which a positive photoresist, AZ4620, is used to yield contact fingers and carbon electrode arrays (~5 μm high).

In this study, we successfully microfabricated high aspect ratio carbon posts (>10:1) by pyrolyzing SU-8 negative photoresist in a simple, one spin step process. Electrochemical measurements established that these C-MEMS electrodes can be reversibly intercalated with lithium.

### Experimental

A schematic drawing of the C-MEMS fabrication process and typical scanning electron microscopy (SEM) photos of photoresist and carbon structures are shown in Fig. 2. The substrates we used are (1) Si, (2) Si<sub>3</sub>N<sub>4</sub> (2000 Å)/Si, (3) SiO<sub>2</sub> (5000 Å)/Si, and (4) Au (3000 Å)/Ti (200 Å)/SiO<sub>2</sub> (5000 Å)/Si. Ti, Au layers were deposited by electron beam (EB) evaporation methods. A negative tone photoresist with different thickness, NANO SU-8 100, was spin-coated onto those substrates. Two kinds of mask designs were used to generate SU-8 posts: 180 × 180 arrays of circles with 50, 40, 30, and 20 μm diam and center to center distance of 100 μm, and 90 × 90 arrays of circles with a 100 μm diam and center to center spacing of 200 μm. The photolithography process used for SU-8 photoresist patterning, included spin coating, soft bake, near UV exposure, development, and post-bake (*vide infra*). Photoresist-derived C-MEMS architectures were obtained in a two-step pyrolysis process in an open end quartz-tube furnace, in which samples were post-baked in a N<sub>2</sub> atmosphere at 300°C for about 40 min first, then heated in N<sub>2</sub> atmosphere with 2000 standard cubic centimeter per minute (sccm) flow rate up to 900°C. The atmosphere was then changed to forming gas [H<sub>2</sub> (5%)/N<sub>2</sub>] flowing at about 2000 sccm rate. The sample was kept at 900°C for 1 h, then the heater was turned off and the samples were cooled in N<sub>2</sub> atmosphere to room temperature. The heating rate was about 10°C/min.

Two different types of electrodes were studied. One was an unpatterned carbon film, 1.6 μm thick, obtained from AZ 4620 photoresist on SiO<sub>2</sub>/Si. This electrode was designed to serve as a refer-

<sup>z</sup> E-mail: chunleiw@uci.edu

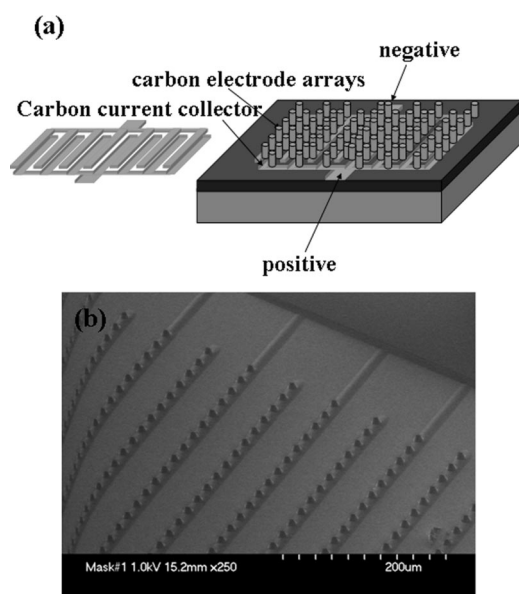


**Figure 1.** Design of C-MEMS 3D microbattery and a typical SEM of low aspect ratio C-MEMS battery arrays. Both the electrodes and contact fingers are made of carbon.

ence sample to determine whether pyrolyzed SU-8 exhibited electrochemically reversible intercalation/deintercalation of lithium. The second sample was a patterned electrode array obtained from SU-8 photoresist, consisting of  $180 \times 180$  posts with a thickness of  $\sim 150 \mu\text{m}$ , on unpatterned carbon obtained from AZ 4620.

The electrochemical measurements were carried out using a three-electrode Teflon cell that employed an O-ring seal to define the working electrode to  $\sim 6.4 \text{ cm}^2$  (circle of 2.86 cm diam). In this way, the projected areas for both types of electrodes were identical. The carbon electrodes served as the working electrode while lithium ribbon (99.9% pure, Aldrich) was used as both the counter and reference electrode. The electrolyte was 1 M  $\text{LiClO}_4$  in a 1:1 volume mixture of ethylene carbonate (EC) and dimethyl carbonate (DMC). All the cells were assembled and tested in an argon filled glove box in which both the oxygen and moisture levels were less than 1 ppm. Galvanostatic and voltammetry experiments were carried out on both types of cells. For the galvanostatic measurements, the current was based on the C/5 rate for graphite (corresponding to 50 and 580  $\mu\text{A}$  for unpatterned and patterned films, respectively) and cells were cycled between 10 mV and 1 V vs.  $\text{Li/Li}^+$ . The voltammetry experi-

ments were carried out using a sweep rate of 0.1 mV/s over the potential range 10 mV to 2 V vs.  $\text{Li/Li}^+$ . All the electrochemical measurements were performed with a computer-controlled Arbin multi-channel station. A Hitachi S-4700-2 field-emission SEM (FESEM) was used to characterize the C-MEMS structures.

## Results and Discussion

Traditionally, photoresist layers in the 50 to 100  $\mu\text{m}$  and beyond range were challenging to formulate, especially in a positive tone. That is, it is very difficult to design a positive tone chemistry to achieve the necessary transparency and to achieve reasonable exposure doses while maintaining excellent sidewall angles.<sup>8,9</sup> Very thick positive Novolak photoresists also have the characteristic of popping or forming voids after exposure as a result of the nitrogen generated during exposure. Furthermore, positive photoresists require as many as three coats to achieve a thickness of  $\sim 65 \mu\text{m}$ .<sup>8</sup> The LIGA process in which PMMA resist is exposed with an X-ray source has demonstrated structures of the order of 1 mm deep.<sup>10</sup> However, this technique requires an expensive synchrotron source, hence the motivation for a cheaper and easier process based on deep UV resist technology. One of the most popular deep UV thick photoresists is a chemically amplified, high-contrast, epoxy-based SU-8 series negative tone photoresist. SU-8 has high optical transparency, which makes it ideally suited for imaging near vertical sidewalls in thick films. SU-8 is best suited for permanent applications, where it is imaged, cured and left in place because this negative photoresist is difficult to remove due to its chemical composition. A potential problem with the use of negative photoresists for the fabrication of C-MEMS structures is their oxygen sensitivity, as the presence of oxygen inhibits cross-linking.<sup>10-12</sup> In the initial attempts to pyrolyze negative photoresists in an oxygen free environment we often found that the structure tended to burn rather than pyrolyze due to the dissolved oxygen remaining in the negative resist. In this work, by carefully controlling pyrolysis condition (as discussed below), we overcame this problem.

As shown in Fig. 2A, a typical SU-8 array of posts on  $\text{Au/Ti/SiO}_2/\text{Si}$  is uniform with straight walls and good edge profiles. The average height of the posts shown here is around  $340 \pm 10 \mu\text{m}$  and the average thickness in the midsection of the posts (*i.e.*, the rod diameter) is  $50 \pm 2 \mu\text{m}$ . After pyrolysis, the overall structure of the cylindrical posts is largely retained, as shown in Fig. 2B. The height: width ratio (midsection of the posts) of the pyrolyzed material corresponds to an aspect ratio of 9.4:1, and we are able to make this ratio as high as 20:1 in a one-step process and 40:1 in a two step process.

Typical SEMs of carbon posts fabricated on different substrates and with different mask designs are shown in Fig. 3. The posts have shrunk much less during the pyrolysis process near the base of the structures than at the midsection due to the good adhesion of SU-8 to the substrate. The tops of the SU-8 posts have shrunk a little less than the midsection as well, perhaps due to overexposure. Shrinkage of the posts is dependent on height. For SU-8 samples whose post heights ranged from 100 to 350  $\mu\text{m}$ , after pyrolysis, the corresponding carbon posts varied from 80 to 275  $\mu\text{m}$ . The large variation in the shrinkage of the posts clearly indicates the fact that different heights and sizes of SU-8 patterns induce different amounts of shrinkage during pyrolysis. In our previous work on AZ 4330, a positive photoresist, the average vertical shrinkage was around 74% while only minor lateral changes occurred after pyrolysis.<sup>5</sup> The minimal lateral shrinkage in this case is partially due to the fact that the positive photoresist structures we made are much thinner and, even for SU-8, close to the surface lateral shrinkage is much less. Compared with positive photoresist, SU-8 gave less vertical shrinkage as well as better adhesion after pyrolysis.

Despite the good adhesion of SU-8, our post patterns peeled from the substrate when using a one step pyrolysis process at 900°C in a vacuum furnace. This problem was finally solved when we switched to the two step pyrolysis procedure in  $\text{N}_2$ /forming gas as described above. The better results are most likely due to the fol-

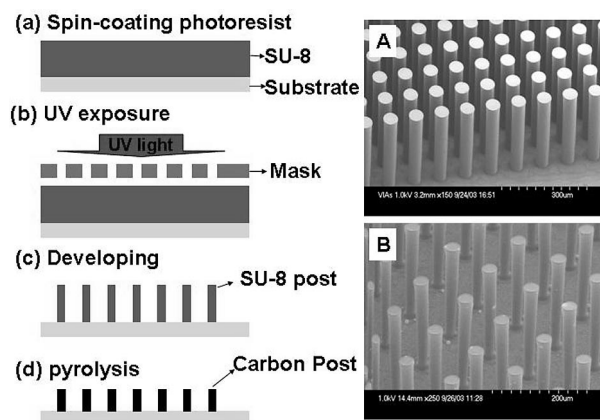


**Figure 2.** A schematic drawing of C-MEMS fabrication process and typical SEM (A) before pyrolysis and (B) after pyrolysis.

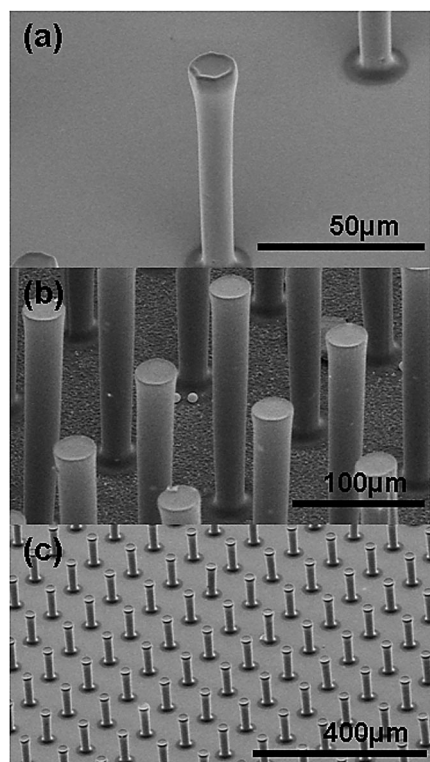


**Figure 3.** Typical SU-8 post arrays after pyrolysis on different substrates with different features: (a) SiN,  $\text{\O}20\ \mu\text{m}$ , C-C:  $100\ \mu\text{m}$ ; (b) Au/Ti/SiO<sub>2</sub>/Si,  $\text{\O}50\ \mu\text{m}$ , C-C:  $100\ \mu\text{m}$ , and (c) SiN,  $\text{\O}30\ \mu\text{m}$ , C-C:  $100\ \mu\text{m}$ .

lowing contributions: the post-bake process cross-links the SU-8 better, enhancing adhesion of SU-8 to the substrate, and the SU-8 adhesion to the substrate results in tensile stress in the carbon posts near the interface and the two-step heating process with its slow heating rate releases this stress more effectively. Another consideration is that slower degassing occurs in a forming gas atmosphere. Heat-treatment during cross-linking generates gaseous byproducts and subsequent outgassing may cause the formation of microcracks which disintegrate the sample. In vacuum, this outgassing would tend to be faster and thus more destructive.<sup>11</sup>

The pyrolyzed SU-8 exhibits reversible intercalation/deintercalation of lithium. In nonpatterned films, the electrochemical behavior is similar to that of coke electrodes with no evidence of staging plateaus and a sloping profile.<sup>13,14</sup> The voltammetric sweep (not shown) is analogous to that reported by Ma *et al.* with some evidence of electrolyte decomposition at near 0.8 V, most of the Li<sup>+</sup> intercalation occurring below 0.5 V and a broad deintercalation peak centered at 0.3 V.<sup>15</sup> The galvanostatic measurements of the unpatterned film show a large irreversible capacity on the first discharge followed by good cycling behavior, which is also consistent with the behavior of coke. In this paper, we characterize the galvanostatic results by normalizing the lithium capacity to the effective electrode area ( $6.4\ \text{cm}^2$ ), *i.e.*, the areal footprint of the electrode. For the second and subsequent cycles, this value is determined to be  $0.070\ \text{mAh cm}^{-2}$  for the second and subsequent cycles. We can estimate a gravimetric capacity for the unpatterned electrode by knowing the film thickness and density. For a fully dense film, this corresponds to  $\sim 220\ \text{mAh g}^{-1}$ , which is within the range of reversible capacities reported for coke.<sup>16</sup>

The patterned carbon electrode exhibits the same general electrochemical behavior. The cyclic voltammogram (CV) in Fig. 4b, for cycles two and three, is virtually identical to that of the unpatterned film electrode. The shoulder at 0.8 V is more pronounced but all other features are the same. Thus, there is no question that the C-MEMS electrode array is electrochemically reversible for lithium

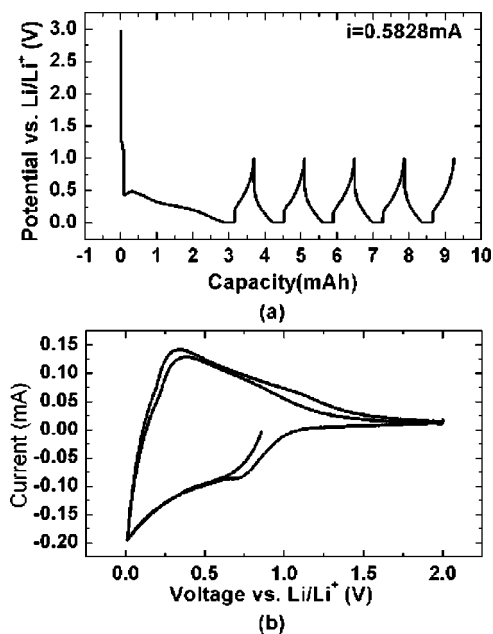


**Figure 4.** (a) Galvanostatic charge/discharge cycle behavior of patterned carbon arrays. (b) CV of patterned carbon arrays.

and that the characteristics of the pyrolyzed SU-8 array are similar to that of coke. The galvanostatic measurements (Fig. 4a) show an irreversible capacity loss on first discharge. For the second and succeeding cycles, the lithium capacity, normalized to the  $6.4\ \text{cm}^2$  areal footprint of the electrode array, is  $0.125\ \text{mAh cm}^{-2}$ . These results indicate that the three-dimensional C-MEMS electrode array possesses nearly 80% higher capacity than that of two-dimensional unpatterned carbon film, for the same defined working electrode area of  $6.4\ \text{cm}^2$ . The reason for the greater capacity arises from the additional active volume of the carbon posts.

Note that the C-MEMS array has a higher internal resistance leading to a significant overpotential, which can be seen in the voltage steps at the beginning of each charge/discharge (Fig. 4a). This higher resistance arises from the fact that the height of the posts is nearly two orders of magnitude larger than the thickness of the unpatterned film. By applying smaller currents, the overpotential can be reduced significantly and the capacity increases. We will report the detailed comparisons of 2D and 3D electrode structures in a future publication.

## Conclusions

We successfully achieved high aspect ratio carbon posts ( $>10:1$ ) by pyrolyzing SU-8 negative photoresist in a simple one spin step process. These C-MEMS array electrodes exhibit reversible intercalation/deintercalation of lithium. The higher lithium capacity obtained for the C-MEMS electrode array suggests that C-MEMS constitutes a powerful approach to building 3D carbon microelectrode arrays for microbattery applications. Such arrays may be connected with C-MEMS leads and enable switching to high voltage or high current depending on the application at hand.

## Acknowledgments

Y.Y. and B.D. greatly appreciate the support of the research by the DoD Multidisciplinary University Research Initiative (MURI) program administered by the Office of Naval Research under grant N00014-01-1-0757 and the Office of Naval Research.

*The University of California assisted in meeting the publication costs of this article.*

## References

1. M. Balkanski, *Sol. Energy Mater. Sol. Cells*, **62**, 21 (2000).
2. K. Kinoshita, in *Handbook of Battery Materials*, J. O. Besenhard, Editor, p. 231, Wiley-VCH, Weinheim (1999).
3. R. W. Hart, H. S. White, B. Dunn, and D. R. Rolison, *Electrochem. Commun.*, **5**, 120 (2003).
4. J. W. Long, B. Dunn, D. R. Rolison, and H. S. White, *Chem. Rev.* (Washington, D.C.), Submitted.
5. S. Ranganathan, R. McCreery, S. M. Majji, and M. Madou, *J. Electrochem. Soc.*, **147**, 277 (2000).
6. K. Kinoshita, X. Song, J. Kim, and M. Inaba, *J. Power Sources*, **81-82**, 170 (1999).
7. J. Kim, X. Song, K. Kinoshita, M. Madou, and R. White, *J. Electrochem. Soc.*, **145**, 2314 (1998).
8. B. E. J. Alderman, C. M. Mann, M. L. Oldfield, and J. M. Chamberlain, *J. Micro-mech. Microeng.*, **10**, 334 (2000).
9. M. C. Peterman, P. Huie, D. M. Bloom, and H. A. Fishman, *J. Micromech. Microeng.*, **13**, 380 (2003).
10. Marc Madou, *Fundamentals of Microfabrication*, CRC Press, Boca Raton, FL (1997).
11. L. A. Liew, W. Zhang, V. M. Bright, L. An, M. L. Dunn, and R. Raj, *Sens. Actuators, A*, **89**, 64 (2001).
12. J. M. Shaw, J. D. Gelorme, N. C. Labianca, W. E. Conley, and S. J. Holmes, *IBM J. Res. Dev.*, **41**, 3 (1997).
13. K. Kinoshita and K. Zaghbi, *J. Power Sources*, **110**, 416 (2002).
14. S. Megahed and B. Scrosati, *J. Power Sources*, **51**, 79 (1994).
15. S. Ma, J. Li, X. Jing, and F. Wang, *Solid State Ionics*, **86-88**, 911 (1996).
16. H. Shi, *J. Power Sources*, **75**, 64 (1998).